JACS
JOURNAL OF THE AMERICAN CHEMICAL SOCIETY

Communication

pubs.acs.org/JACS

Modulating Nanoparticle Superlattice Structure Using Proteins with Tunable Bond Distributions

Janet R. McMillan,[†,‡] Jeffrey D. Brodin,[†,‡] Jaime A. Millan,[§,‡] Byeongdu Lee,[∥] Monica Olvera de la Cruz,[†,§,‡] and Chad A. Mirkin*[,†,§,‡]

[†]Department of Chemistry, [§]Department of Materials Science and Engineering, and [‡]International Institute for Nanotechnology, Northwestern University, 2145 Sheridan Road, Evanston, Illinois 60208, United States

[∥]X-ray Science Division, Argonne National Laboratory, Argonne, Illinois 60439, United States

Supporting Information

ABSTRACT: Herein, we investigate the use of proteins with tunable DNA modification distributions to modulate nanoparticle superlattice structure. Using beta-galactosidase (*β*gal) as a model system, we have employed the orthogonal chemical reactivities of surface amines and thiols to synthesize protein−DNA conjugates with 36 evenly distributed or 8 specifically positioned oligonucleotides. When these are assembled into crystalline superlattices with gold nanoparticles, we find that the distribution of DNA modifications modulates the favored structure: *β*gal with uniformly distributed DNA bonding elements results in body-centered cubic crystals, whereas DNA functionalization of cysteines results in AB_2 packing. We probe the role of protein oligonucleotide number and conjugate size on this observation, which revealed the importance of oligonucleotide distribution in this observed assembly behavior. These results indicate that proteins with defined DNA modification patterns are powerful tools for controlling nanoparticle superlattices architecture, and establish the importance of oligonucleotide distribution in the assembly behavior of protein−DNA conjugates.

Programming the assembly of nanoscale building blocks into supramolecular architectures presents a formidable chemical challenge and a potentially powerful strategy for the bottom-up construction of functional macroscopic materials. Over the past two decades, DNA has emerged as a valuable tool for realizing this goal,[1] where nanoscale building blocks can be functionalized with oligonucleotides that act as bonding elements to mediate particle assembly into crystalline superlattices.[2] These materials can be engineered with precise control over interparticle spacing, lattice symmetry,[3] bond strength,[4] particle composition,[5] and shape[6] and designed to respond to various stimuli.[7] The synthesis of binary superlattices composed of hard and soft material building blocks, such as gold nanoparticles (AuNPs) and hollow cross-linked particles,[8] or DNA nanostructure frameworks[9] has dramatically expanded the library of structures accessible in these systems. In particular, the incorporation of proteins in nanoparticle superlattices has provided new opportunities to engineer structural diversity and function into these materials that cannot be achieved with nanoparticles or other soft material building blocks alone.[5b] The well-defined, tunable, and chemically anisotropic surfaces of proteins offer the possibility of finely controlling the number and position of oligonucleotide surface modifications to an extent not possible with current physical and chemical approaches to anisotropically functionalize nanoparticle surfaces.[10] Currently, however, only proteins densely functionalized with DNA through their surface lysine residues have been studied in nanoparticle superlattices,[5b] while the assembly of proteins with specifically positioned oligonucleotides remains unexplored. Ultimately, by studying the assembly properties of proteins with variable oligonucleotide distributions, we may elucidate design rules for controlling structural outcomes that provide a strong complement to other methods for engineering protein lattices[11] and binary materials.[12] Toward this goal, we utilized the orthogonal reactivities of surface amines and thiols to synthesize protein−DNA conjugates with variable distributions of oligonucleotides and studied their assembly in nanoparticle superlattices.

Herein, we investigate the assembly of spherical DNA-functionalized AuNPs (10 nm diameter) with the tetrameric enzyme beta-galactosidase (*β*gal; with dimensions of 17 × 12 × 8 nm, Figure S11) modified with complementary DNA either through its 36 evenly distributed surface lysine (amine) residues (*β*gal-1) or through its 8 cysteine (thiol) residues (*β*gal-2), located at the top and bottom faces of each of the four corners of the protein (Figure 1). By modulating the residue of attachment, the oligonucleotide number, distribution, and hydrodynamic radius (HDR) of the protein conjugate are varied. Based on our knowledge of the assembly of isotropically functionalized nanoparticles,[3] we anticipated that the favored arrangement of AuNPs around each protein−DNA conjugate will differ due to their varying oligonucleotide number or HDR. Additionally, we hypothesized that the spatial distribution of bonding oligonucleotides on the protein surface could also represent an important factor in dictating the assembly behavior of these building blocks. By elucidating the roles of these three parameters in the assembly of this fundamentally new class of building blocks, we demonstrate that the distribution of "bonding" oligonucleotides on the protein−DNA conjugates has a significant effect on the assembly behavior of AuNPs.

We first used orthogonal chemistries to label the 36 solvent-accessible amines or 8 thiols of *β*gal with DNA to yield our

Received: November 17, 2016
Published: January 25, 2017

DOI: 10.1021/jacs.6b11893
J. Am. Chem. Soc. 2017, 139, 1754−1757

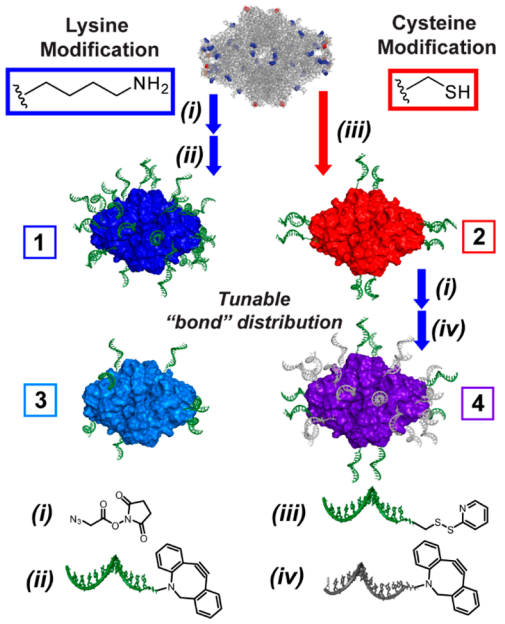

Figure 1. βgal-DNA conjugates with variable DNA distributions synthesized by addressing lysine (blue) or cysteine residues (red). Left: synthesis of βgal-1 and -3 using an NHS-N3 (i) linker and DBCO–DNA (ii). Right: synthesis of βgal-2 using pyridyl disulfide-terminated DNA (iii). βgal-4 is synthesized by further reacting the amine residues of βgal-2 with T18 DBCO-terminated oligonucleotide (iv).

desired building blocks, βgal-1 and βgal-2. Native βgal was labeled using a maleimide (βgal-1) or *N*-hydroxysuccinimide (βgal-2) cyanine 5 (Cy5) fluorophore to enable quantification of protein concentration after DNA attachment (Supporting Information (SI), section 2.1). βgal-1 was prepared by adapting a previous approach,[5b,13] wherein an NHS ester-azide linker (Figure 1 (i)) was reacted with Cy5-modified βgal, functionalizing exposed lysine residues with azide groups (38/tetramer; Figure S2). Subsequently, DNA with a 5′ dibenzocyclooctyne (DBCO) modification (Figure 1 (ii)) was reacted with azide-modified βgal through a strain-promoted cycloaddition reaction.[14] Separately, βgal-2 was prepared by reacting βgal-Cy5 with 5′ pyridyl disulfide-terminated DNA (Figure 1 (iii)). After purification, UV–vis spectroscopy was used to quantify the number of DNA strands on each orthogonally functionalized construct. The resulting spectra showed 36 strands/tetramer for βgal-1 and 8 strands/tetramer for βgal-2, consistent with the number of solvent-accessible residues of each type (Figure S4), while circular dichroism (CD) spectroscopy indicated that the secondary structure of the protein is maintained after each modification procedure (Figure S5). Further, size exclusion chromatography confirmed the covalent attachment of oligonucleotides and the preservation of the tetrameric quaternary structure of the conjugates, and also confirmed that βgal-2 had a smaller HDR than βgal-1 as a result of the decreased number of surface-conjugated strands (Figure S7). To further support the preservation of the native structure of each modified enzyme, the catalytic efficiencies of each βgal-DNA conjugate were compared to that of native βgal. Using a substrate analogue, *o*-nitrophenyl-β-D-galactopyranoside, we found that k_{cat}/K_m values were similar for both DNA- and azide-modified βgal (Figure S10, Table S2). Overall, our characterization results are consistent with the selective oligonucleotide labeling of solvent-accessible lysines and cysteines and the preservation of the native βgal structure.

Next, we prepared binary superlattices of βgal-1 and βgal-2 with 10 nm AuNPs to investigate the phase behavior of the AuNPs with each protein conjugate, testing our hypothesis that altering the residue of DNA attachment will change the favored AuNP arrangement around βgal. This was done by combining the protein and AuNP building blocks with linking strands containing a complementary 6-base-pair single-stranded overhang at the 5′ terminus (Figure 2A). The combination of the AuNP and protein building blocks with their hybridized linking strands induced the precipitation of aggregates, which were then heated beyond their dissociation temperature (Figure S12) and slowly cooled (0.01 °C/min) to allow the system to reorganize into its thermodynamically favored configuration.[15]

Synchrotron-based small-angle X-ray scattering (SAXS) was used to probe the arrangement of the AuNPs in the resulting assemblies. Due to the large difference in electron density between AuNPs and proteins, SAXS provides information exclusively on AuNP position. In general with DNA-mediated nanoparticle crystallization, a lattice will form wherein the number of DNA-hybridization events between neighboring

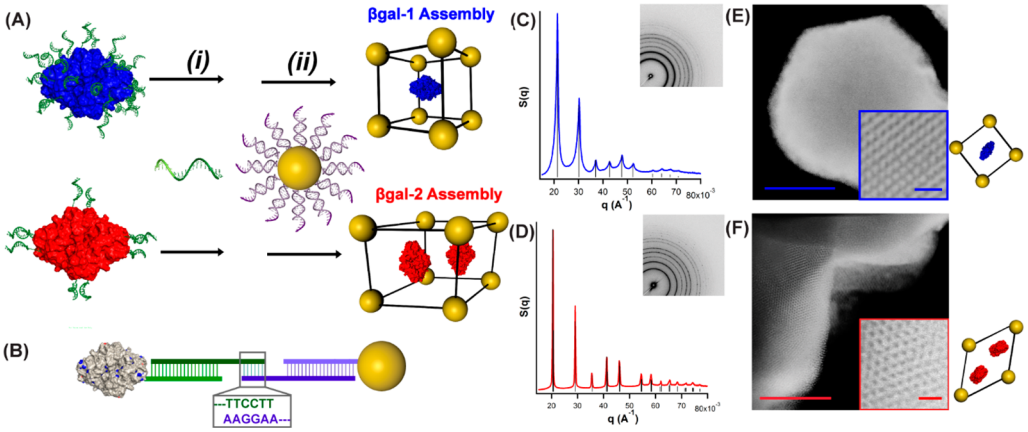

Figure 2. Assembly and characterization of AuNP superlattices with βgal-1 (top) and βgal-2 (bottom). (A) Assembly scheme for binary superlattices showing (i) linker addition and (ii) AuNP addition. (B) Schematic of protein and AuNP with their hybridized linker strands (only one DNA duplex shown for clarity). (C,D) SAXS patterns of binary superlattices prepared from βgal-1 and -2, respectively, with expected reflections in black. (E) STEM images of simple cubic superlattice. Scale bar = 1 μm (50 nm inset). (F) STEM images of simple hexagonal superlattices. Scale bar = 0.5 μm (50 nm inset), with top view ((0 0 1) plane) of the unit cells shown.

DOI: 10.1021/jacs.6b11893
J. Am. Chem. Soc. 2017, 139, 1754–1757

particles is maximized.[3] According to this principle, two complementary, isotropically functionalized particles of similar size favor a CsCl-type lattice. Indeed, SAXS data revealed, as expected, that isotropically functionalized βgal-1 templated a simple cubic arrangement of AuNPs (Figure 2C). Here, the nonspherical shape of the protein does not influence the observed nanoparticle symmetry, likely due to the large ratio of DNA length to protein size (Figure S11).[6a] In contrast, a simple hexagonal arrangement of AuNPs was found with βgal-2 via SAXS and scanning transmission electron microscopy (STEM) imaging (Figure 2D,F), supporting our hypothesis that altering the residue of oligonucleotide attachment on βgal will change the favored arrangement of complementary AuNPs. To elucidate the structure of this simple hexagonal AuNP arrangement with respect to the protein, we measured the stoichiometry of each component in the lattice using a combination of UV−vis and fluorescence spectroscopic quantification of AuNP and protein concentration, respectively. These results revealed a 2:1 lattice stoichiometry, indicating an AB_2 packing arrangement (Figure S15).

AB_2 structures have been previously observed in nanoparticle superlattice systems when two components have hydrodynamic radii that differ by more than a factor of ∼1.5, whereas only CsCl packing has been observed with particles of similar size. In addition, for dissimilar particle sizes, AB_2 structures become favored over CsCl packing when the number of oligonucleotides of the smaller particles is lower than that of the larger particle.[3] To understand the origin of the observed AB_2 packing with βgal-2, and elucidate the role of protein oligonucleotide distribution in dictating assembly behavior, we investigated the effect of protein HDR and linker number on the observed AuNP structure. First, to probe the effect of HDR, we synthesized βgal-4, a conjugate with an identical number and distribution of bonding oligonucleotides as βgal-2, but with a HDR similar to that of βgal-1. We synthesized this conjugate by further functionalizing the amine residues of βgal-2 with a poly-T oligonucleotide (Figure 1), and characterized the conjugate as previously described (Figures S4, S5, S7, and S10). Upon assembly of βgal-4 with complementary AuNPs, we observed a simple hexagonal AuNP structure via SAXS (Figure 3A), with a lattice expansion of 8% along the *a* axis and 6% along the *c* axis, consistent with the increasing HDR of the protein arising from a greater number of DNA surface ligands. Therefore, the smaller HDR of βgal-2 as compared to βgal-1 is not an important factor for our observation of the AB_2 structure.

Next, to investigate the effect of linker number on the assembly of βgal, we synthesized a conjugate having an average of eight oligonucleotides randomly distributed on its surface lysine residues (βgal-3) by adding 10 equivalents of DBCO-terminated DNA to azide-modified βgal. When this conjugate was assembled, SAXS and STEM revealed mostly disordered aggregates among more ordered domains, corresponding to a simple hexagonal AuNP arrangement (Figure 3B,D). Thus, a low number of protein-conjugated oligonucleotides favors a more densely packed AB_2 structure, a result consistent with observations made in nanoparticle systems;[3] however, the fact that βgal-3 results in a highly disordered structure indicates that the six bonds between the protein and its six nearest AuNPs are not well defined. Our observations indicate that the defined position and number of oligonucleotides accessible by chemically addressing cysteine residues is necessary for the formation of highly ordered AB_2 binary crystals. Further, in the case of βgal-3, since not all of the reactive surface residues are being

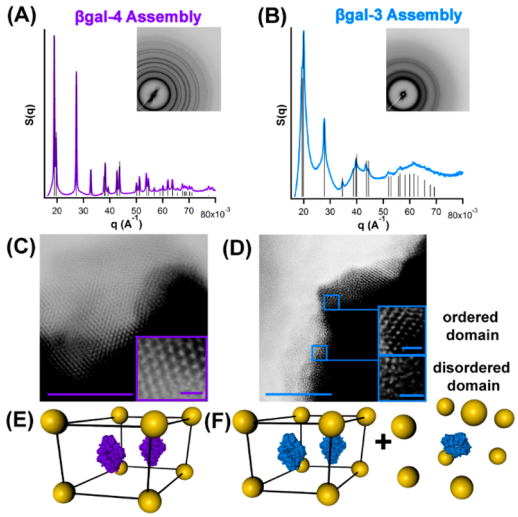

Figure 3. Characterization of AuNP superlattices with βgal-4 (left) and βgal-3 (right). (A) SAXS pattern of βgal-4-AuNP assembly shows a simple hexagonal AuNP arrangement. (B) SAXS pattern of βgal-3 shows domains of AB_2 ordering. (C,D) EM images of βgal-4- and βgal-3-AuNP assemblies. Scale bars = 0.5 μm (50 nm inset). (E,F) Schematics of unit cells of βgal-4- and -3-AuNP assemblies.

functionalized, it is possible that the distribution of oligonucleotide number and position between proteins within a sample is also a contributing factor to the observed lack of long-range order.[16] Regardless, it is clear that the number as well as the defined positional distribution of bonding elements in the case of βgal-2 drives the formation of highly ordered AB_2 crystals.

To gain further insight into the system, coarse-grained isobaric (NPT) molecular dynamics simulations were performed on the βgal-2 system at zero pressure, starting from an ideally constructed AB_2 lattice, with proteins randomly oriented (see SI, section S7 for additional description).[17] Simulations confirmed that the proposed AB_2 packing was stable and allowed all protein oligonucleotides to hybridize to neighboring AuNPs. Interestingly, upon equilibration, the proteins showed a clear trend to orient with their longest dimension along the *c*-axis of the unit cell, with 61% of the proteins having their long axis oriented between 0° and 40° with respect to the *c*-axis of the unit cell (Figure S19), suggesting that the specific placement of DNA on the protein surface plays a role in the quality of the lattice observed.

Herein, we have elucidated oligonucleotide "bond" distribution on a protein core as an important factor in directing its co-crystallization with AuNPs. We have presented a strategy for positioning oligonucleotides on protein surfaces using their specific chemical topology, enabling conjugate "bond" number, position, and HDR to be varied independently. We have elucidated the role of these factors in terms of assembly outcome and demonstrated the importance of oligonucleotide distribution on protein surfaces in directing their crystallization into macroscopic materials. We anticipate that using site-specific mutagenesis to rationally tune the number and position of chemically addressable surface residues, and thereby oligonucleotides, in addition to our ability to conjugate multiple orthogonal oligonucleotide sequences to a single building block, will enable a high degree of control over their assembly into discrete and 1-, 2-, and 3-dimensional morphologies, with precise control over protein spacing and interaction strength enabled by the use of DNA hybridization interactions. Further, this approach

DOI: 10.1021/jacs.6b11893
J. Am. Chem. Soc. 2017, 139, 1754−1757

will enable combining multiple proteins, or proteins and nanomaterials with complementary functionalities, toward realizing multicomponent materials with applications ranging from catalysis to sensing.

■ ASSOCIATED CONTENT

Supporting Information

The Supporting Information is available free of charge on the ACS Publications website at DOI: 10.1021/jacs.6b11893.

Methods, Tables S1−S5, and Figures S1−S19 (PDF)

■ AUTHOR INFORMATION

Corresponding Author

*chadnano@northwestern.edu

ORCID

Byeongdu Lee: 0000-0003-2514-8805

Chad A. Mirkin: 0000-0002-6634-7627

Notes

The authors declare no competing financial interest.

■ ACKNOWLEDGMENTS

This material is based upon work supported by the U.S. Department of Defense National Security Science and Engineering Faculty Fellowship (award N00014-15-1-0043) and the AFOSR (award FA9550-11-1-0275). SAXS experiments were carried out at the Dupont−Northwestern−Dow Collaborative Access Team beamline at the Advanced Photon Source (APS) at Argonne National Laboratory, and use of the APS was supported by the U.S. Department of Energy (DE-AC02-06CH11357). This work made use of the EPIC facility of Northwestern University's NUANCE Center, which has received support from the Soft and Hybrid Nanotechnology Experimental (SHyNE) Resource (NSF NNCI-1542205); the MRSEC program (NSF DMR-1121262) at the Materials Research Center; the International Institute for Nanotechnology (IIN); the Keck Foundation; and the State of Illinois, through the IIN. J.A.M. is supported by an IIN Fellowship, the Center for Computation and Theory of Soft Materials at Northwestern University, and NSF award DMR-1611076. J.R.M. gratefully acknowledges the National Science and Engineering Research Council of Canada for a Postgraduate Fellowship.

■ REFERENCES

(1) (a) Mirkin, C. A.; Letsinger, R. L.; Mucic, R. C.; Storhoff, J. J. *Nature* **1996**, *382*, 607−609. (b) Seeman, N. C. *Nature* **2003**, *421*, 427−431. (c) Rothemund, P. W. K. *Nature* **2006**, *440*, 297−302. (d) Jones, M. R.; Seeman, N. C.; Mirkin, C. A. *Science* **2015**, *347*, 1260901.

(2) (a) Nykypanchuk, D.; Maye, M. M.; van der Lelie, D.; Gang, O. *Nature* **2008**, *451*, 549−552. (b) Park, S. Y.; Lytton-Jean, A. K. R.; Lee, B.; Weigand, S.; Schatz, G. C.; Mirkin, C. A. *Nature* **2008**, *451*, 553−556.

(3) Macfarlane, R. J.; Lee, B.; Jones, M. R.; Harris, N.; Schatz, G. C.; Mirkin, C. A. *Science* **2011**, *334*, 204−208.

(4) (a) Pal, S.; Zhang, Y.; Kumar, S. K.; Gang, O. *J. Am. Chem. Soc.* **2015**, *137*, 4030−4033. (b) Thaner, R. V.; Eryazici, I.; Macfarlane, R. J.; Brown, K. A.; Lee, B.; Nguyen, S. T.; Mirkin, C. A. *J. Am. Chem. Soc.* **2016**, *138*, 6119−6122.

(5) (a) Zhang, C.; Macfarlane, R. J.; Young, K. L.; Choi, C. H. J.; Hao, L.; Auyeung, E.; Liu, G.; Zhou, X.; Mirkin, C. A. *Nat. Mater.* **2013**, *12*, 741−746. (b) Brodin, J. D.; Auyeung, E.; Mirkin, C. A. *Proc. Natl. Acad. Sci. U. S. A.* **2015**, *112*, 4564−4569.

(6) (a) Jones, M. R.; Macfarlane, R. J.; Lee, B.; Zhang, J.; Young, K. L.; Senesi, A. J.; Mirkin, C. A. *Nat. Mater.* **2010**, *9*, 913−917. (b) Lu, F.; Yager, K. G.; Zhang, Y.; Xin, H.; Gang, O. *Nat. Commun.* **2015**, *6*, 6912.

(7) (a) Barnaby, S. N.; Thaner, R. V.; Ross, M. B.; Brown, K. A.; Schatz, G. C.; Mirkin, C. A. *J. Am. Chem. Soc.* **2015**, *137*, 13566−13571. (b) Kim, Y.; Macfarlane, R. J.; Jones, M. R.; Mirkin, C. A. *Science* **2016**, *351*, 579−582.

(8) Auyeung, E.; Cutler, J. I.; Macfarlane, R. J.; Jones, M. R.; Wu, J.; Liu, G.; Zhang, K.; Osberg, K. D.; Mirkin, C. A. *Nat. Nanotechnol.* **2012**, *7*, 24−28.

(9) (a) Liu, W.; Tagawa, M.; Xin, H. L.; Wang, T.; Emamy, H.; Li, H.; Yager, K. G.; Starr, F. W.; Tkachenko, A. V.; Gang, O. *Science* **2016**, *351*, 582−586. (b) Tian, Y.; Zhang, Y.; Wang, T.; Xin, H. L.; Li, H.; Gang, O. *Nat. Mater.* **2016**, *15*, 654−661.

(10) (a) Martin, B. R.; Dermody, D. J.; Reiss, B. D.; Fang, M.; Lyon, L. A.; Natan, M. J.; Mallouk, T. E. *Adv. Mater.* **1999**, *11*, 1021−1025. (b) Roh, K.-H.; Martin, D. C.; Lahann, J. *Nat. Mater.* **2005**, *4*, 759−763. (c) Xu, X.; Rosi, N. L.; Wang, Y.; Huo, F.; Mirkin, C. A. *J. Am. Chem. Soc.* **2006**, *128*, 9286−9287. (d) Groschel, A. H.; Walther, A.; Lobling, T. I.; Schacher, F. H.; Schmalz, H.; Muller, A. H. E. *Nature* **2013**, *503*, 247−251. (e) Edwardson, T. G. W.; Lau, K. L.; Bousmail, D.; Serpell, C. J.; Sleiman, H. F. *Nat. Chem.* **2016**, *8*, 162−170.

(11) (a) Dotan, N.; Arad, D.; Frolow, F.; Freeman, A. *Angew. Chem., Int. Ed.* **1999**, *38*, 2363−2366. (b) Lanci, C. J.; MacDermaid, C. M.; Kang, S.-g.; Acharya, R.; North, B.; Yang, X.; Qiu, X. J.; DeGrado, W. F.; Saven, J. G. *Proc. Natl. Acad. Sci. U. S. A.* **2012**, *109*, 7304−7309. (c) Sakai, F.; Yang, G.; Weiss, M. S.; Liu, Y.; Chen, G.; Jiang, M. *Nat. Commun.* **2014**, *5*, 4634. (d) Sontz, P. A.; Bailey, J. B.; Ahn, S.; Tezcan, F. A. *J. Am. Chem. Soc.* **2015**, *137*, 11598−11601. (e) Gonen, S.; DiMaio, F.; Gonen, T.; Baker, D. *Science* **2015**, *348*, 1365−1368. (f) Suzuki, Y.; Cardone, G.; Restrepo, D.; Zavattieri, P. D.; Baker, T. S.; Tezcan, F. A. *Nature* **2016**, *533*, 369−373.

(12) (a) Kostiainen, M. A.; Hiekkataipale, P.; Laiho, A.; Lemieux, V.; Seitsonen, J.; Ruokolainen, J.; Ceci, P. *Nat. Nanotechnol.* **2013**, *8*, 52−56. (b) Künzle, M.; Eckert, T.; Beck, T. *J. Am. Chem. Soc.* **2016**, *138*, 12731−12734.

(13) Brodin, J. D.; Sprangers, A. J.; McMillan, J. R.; Mirkin, C. A. *J. Am. Chem. Soc.* **2015**, *137*, 14838−14841.

(14) Agard, N. J.; Prescher, J. A.; Bertozzi, C. R. *J. Am. Chem. Soc.* **2004**, *126*, 15046−15047.

(15) Auyeung, E.; Li, T. I. N. G.; Senesi, A. J.; Schmucker, A. L.; Pals, B. C.; de la Cruz, M. O.; Mirkin, C. A. *Nature* **2014**, *505*, 73−77.

(16) Mullen, D. G.; Banaszak Holl, M. M. *Acc. Chem. Res.* **2011**, *44*, 1135−1145.

(17) Li, T. I. N. G.; Sknepnek, R.; Macfarlane, R. J.; Mirkin, C. A.; Olvera de la Cruz, M. *Nano Lett.* **2012**, *12*, 2509−2514.

DOI: 10.1021/jacs.6b11893
J. Am. Chem. Soc. 2017, 139, 1754−1757